1914–1921 *Nucleic Acids Research, 2013, Vol. 41, No. 3* *Published online 18 December 2012*
doi:10.1093/nar/gks986

Vaccinia and influenza A viruses select rather than adjust tRNAs to optimize translation

Mariana Pavon-Eternod[1], Alexandre David[1], Kimberly Dittmar[2], Peter Berglund[1], Tao Pan[2], Jack R. Bennink[1] and Jonathan W. Yewdell[1,*]

[1]Laboratory of Viral Diseases, National Institute of Allergy and Infectious Diseases, Bethesda, MD 20892 and [2]Department of Biochemistry and Molecular Biology, University of Chicago, Chicago, IL 60637, USA

Received July 31, 2012; Revised September 14, 2012; Accepted September 20, 2012

ABSTRACT

Transfer RNAs (tRNAs) are central to protein synthesis and impact translational speed and fidelity by their abundance. Here we examine the extent to which viruses manipulate tRNA populations to favor translation of their own genes. We study two very different viruses: influenza A virus (IAV), a medium-sized (13 kB genome) RNA virus; and vaccinia virus (VV), a large (200 kB genome) DNA virus. We show that the total cellular tRNA population remains unchanged following viral infection, whereas the polysome-associated tRNA population changes dramatically in a virus-specific manner. The changes in polysome-associated tRNA levels reflect the codon usage of viral genes, suggesting the existence of local tRNA pools optimized for viral translation.

INTRODUCTION

Viruses are wholly dependent on the host translation machinery to synthesize their proteins. Consequently, viral codon usage is thought to be under selective pressure to adapt to the host cell transfer RNA (tRNA) pool. Since host codon usage generally reflects the host tRNA pool (1,2), viral translation should be most efficient when viral codon usage is similar to that of the host genes. In many cases, however, viral codon usage seems poorly adapted to that of its host (3–5). For example, Influenza A viruses (IAVs) have a GC-poor genome and favor A/U-ending codons (6,7). The reason for this codon bias remains an open question, often approached from an evolutionary perspective. Numerous studies have attributed codon usage bias to translational selection, mutational bias and genetic drift (8–11). Matching viral and host codon usage can enhance translation of viral proteins and increase immunogenicity (12–17).

Host codon usage or tRNA gene copy numbers are frequently used as a proxy for cellular tRNA levels. These proxies are typically highly inaccurate. tRNA levels fluctuate based on cell type and environmental conditions. For example, a study of tissue-specific tRNA expression revealed distinct widely divergent tRNA expression patterns in all tissues examined (18). Distinct tRNA expression patters have been reported in many transformed cell types, including cells transformed by viruses (19–22).

Viruses display a tremendous interest in translation, rapidly altering a number of translational components while shifting translation from host to viral mRNAs (23,24). We reported that infection of cultured human cells with adenovirus, vaccinia virus (VV) or IAV alters tRNA acylation specificity, essentially altering the genetic code (25). These findings prompt the question of whether viruses also modulate tRNA populations to enhance viral protein synthesis.

To answer this question, here we use tRNA microarray technology to measure tRNA levels in cells infected with two completely distinct viruses: IAV, a negative-strand RNA virus and VV, a double-stranded DNA virus.

MATERIALS AND METHODS

Cells and infections

HeLa cells (American Type Culture Collection) were cultured in DMEM supplemented with 7.5% FBS.

IAV infection

HeLa cells were grown to 60–70% confluency and infected with the Influenza A/Puerto Rico/8/34 strain at a multiplicity of 10 in Autopow infection medium, pH 6.6. After

*To whom correspondence should be addressed. Tel: +301 402 4602; Fax: +301 480 4802; Email: jyewdell@nih.gov

The authors wish it to be known that, in their opinion, the first two authors should be regarded as joint First Authors.

adsorption at 37°C for 1 h, infected monolayers were overlaid with DMEM supplemented with 7.5% FBS and incubated for an additional 5 h.

VV infection

HeLa cells were grown to 60–70% confluency and infected with VV WR at a multiplicity of 10 in saline supplemented with 0.1% BSA. After adsorption at 37°C for 1 h, infected monolayers were overlaid with DMEM supplemented with 7.5% FBS and incubated for an additional 5 h.

RNA isolation

Total cellular RNA

Total RNA was extracted from HeLa cells 6 h post-infection by the TRIzol method (Invitrogen).

Polysome RNA

HeLa cells 6 h post-infection were trypsinized in the presence of emetine (25 μg/ml, EMD) and re-suspended in ice-cold polysome lysis buffer (50 mM Tris–HCl pH 7.5, 5 mM $MgCl_2$, 25 mM KCl, 0.2 M sucrose, 1% NP-40, 10 u/ml RNaseOUT). Cell lysate was transferred to Lysing Matrix D tubes (MP Biomedical) and vortexed 1 min at 4°C. The lysate was clarified by spinning 10 min at 14 000 rpm at 4°C. The supernatant was loaded on a sucrose density gradient (15–50% w/v) prepared in SW41 tubes (Beckman) and spun at 4°C, 35 000 rpm for 2.5 h. Sucrose solutions were prepared in gradient buffer (50 mM Tris–HCl pH 7.5, 5 mM $MgCl_2$, 25 mM KCl, 100 μg/ml cycloheximide, 10 u/ml RNaseOUT). Twenty one fractions were collected manually from the top of the gradient and the OD260 of each fraction measured by nanodrop (Thermo Scientific). The polysome fractions were pooled and centrifuged for 2 h at 40 000 rpm in T100.1 tubes to pellet the ribosomes. Polysome RNA was then extracted from the ribosome pellet following the TRIzol method (Invitrogen).

tRNA microarrays

The tRNA microarray experiment consists of four steps starting from total or polysome RNA: (i) deacylation to remove any amino acids still attached to the tRNA; (ii) selective fluorophore labeling of tRNA; (iii) hybridization; and (iv) data analysis. The reproducibility of the tRNA microarray method and result validation by northern blots have been extensively described in previously published papers.

Deacylation

Total or polysome RNA (0.25 μg/μl) was spiked with three tRNA transcript standards (*Escherichia coli* $tRNA^{Lys}$, *E. coli* $tRNA^{Tyr}$ and *Saccharomyces cerevisiae* $tRNA^{Phe}$) at 0.67 pmol each per μg RNA. The mixture was incubated in 100 mM Tris–HCl pH 9.0 at 37°C for 30 min, then neutralized by the addition of an equal volume of 100 mM sodium acetate/acetic acid, 100 mM NaCl at pH 4.8. After ethanol precipitation, deacylated RNA was dissolved in water and its integrity verified by agarose gel electrophoresis.

Fluorophore labeling

tRNA in each sample was selectively labeled with either Cy3 or Alexa647 using an enzymatic ligation method previously described. The labeling oligonucleotide consists of an 8 bp RNA:DNA hybrid helix containing a Cy3 or Alexa647 fluorophore in the loop and an overhang complementary to the 3′CCA nucleotides universally conserved in all tRNAs. The ligation reaction was carried out overnight at 16°C with 1 u/μl T4 DNA ligase (USB Corp) and 9 μM labeling oligonucleotide.

Hybridization

1–2.5 μg of labeled RNA were hybridized on commercially printed custom microarrays (Microarrays Inc.). Hybridization was performed in a DigiLab GeneMachines Hyb4 at 60°C for 16 h. Each sample array was hybridized with an infected sample and uninfected control sample as a reference, labeled with Cy3 or Alexa647. The control array was hybridized with uninfected control sample labeled with Cy3 and Alexa647.

Data analysis

Arrays were scanned using a GenePix 4000b scanner (Axon Instruments). For both Cy3 and Alexa647, PMT gain was set at 600 and power at 100%. These settings were chosen to provide optimal signal without saturation. Array images were generated and analysed using GenePix 6.0 software. GenePix adaptive circle spot segmentation was used for image analysis. To account for differences in labeling and hybridization efficiencies, the following normalization procedure was applied to each probe: (i) average Alexa647/Cy3 ratios were calculated from all the replicate spots for each probe; (ii) the sample array Alexa647/Cy3 ratio was normalized to the corresponding control array Alexa647/Cy3 ratio; and (iii) the obtained value was divided by the average of the Alexa647/Cy3 ratios of the three tRNA standards spiked in at the deacylation step.

S^{35} labeling

HeLa cells were trypsinized and washed twice in methionine-free DMEM (Invitrogen). Approximately 10^6 cells were incubated for 5 min at 37°C in methionine-free DMEM supplemented with 0.1 mCi/ml S^{35}-methionine (Perkin Elmer). Cells were washed twice with ice-cold PBS supplemented with 100 μg/ml cycloheximide and re-suspended in 500 μl lysis buffer (1X PBS, 1% NP-40, Roche Mini Protease Inhibitor). Lysate was incubated on ice for 15 min prior to loading on a NuPAGE 10% Bis-Tris gel (Invitrogen) or TCA precipitation. S^{35}-labeled products were visualized on a phosphorimager (Typhoon, Amersham Biosciences) and analysed using ImageJ software (http://rsbweb.nih.gov/ij/). For TCA precipitation, 5 μl of each sample was applied per spot of a 96-well filter mat (six replicates per sample). After drying at 60°C, the mat was incubated in 10% TCA for 30 min at room temperature and washed twice in 70% ethanol (10 min per wash). The mat was again dried at 60°C and placed in a scintillation bag with 5 ml scintillation liquid (Betaplate Scint, Perkin Elmer). Radioactivity was

quantitated using a liquid scintillation counter (1450 MicroBeta Lux, Perkin Elmer).

tRNA—codon usage analysis

Relative tRNA abundance

Relative tRNA abundances were measured using the tRNA microarray method described above. Our tRNA microarray measurements reflect changes in tRNA abundance relative to the uninfected control sample rather than absolute tRNA abundances because (i) all arrays include the control sample; and (ii) all data are normalized to the control. Only tRNA isoacceptors uniquely detected by one tRNA probe were used for tRNA—codon usage analysis. For example, the three proline tRNA isoacceptors are detected by a single probe on the tRNA microarray and so were excluded from the analysis.

Codon usage

The VV WR (AY243312.1) and IAV A/Puerto Rico/8/34/Mount Sinai (H1N1) (AF389115.1 through AF389122.1) complete sequences were downloaded from NCBI. Coding sequences were extracted and codon usage was calculated using the Sequence Manipulation Suite (version 2, http://www.bioinformatics.org/sms2/). Human codon usage for all human genes was obtained from the Codon Usage Database (http://www.kazusa.or.jp/codon/). Amino acids read by only one codon (e.g. AUG for Met and UGG for Trp) and stop codons were excluded from tRNA—codon usage analysis.

tRNA—codon usage correlations

Viral and human codon usage were expressed as frequency per 1000 codons. Because a given tRNA isoacceptor may decode more than one mRNA codon (wobble), a converted codon usage was used for further analysis. The codon frequencies of all the codons decoded by a given tRNA were added together to obtain the converted codon usage corresponding to that tRNA. Viral converted codon usage was normalized to human converted codon usage, reflecting relative rather than absolute codon usage. This normalization was necessary because the tRNA microarray method provides relative and not absolute tRNA abundances (see above).

Software and data processing

Gel analysis was performed using ImageJ software (http://rsbweb.nih.gov/ij/). All data were plotted using Prism (Graphpad). One sample *t*-tests were performed using GraphPad QuickCalcs (http://graphpad.com/quickcalcs/OneSampleT1.cfm). To apply the Bonferroni correction, the obtained *P*-values were divided by the number of events measured.

RESULTS AND DISCUSSION

Codon usages of influenza A and VV genes differ from human genes

Viral codon adaptation is considered poor when codons that are infrequent in host genes are enriched in viral genes. In this study, we used two viruses distinct from each other in almost every aspect of their genome and replication cycle: IAV and VV. IAV is a negative-stranded RNA virus with a limited genome (13 kB) that replicates its RNA in the nucleus, where it steals caps from cellular mRNAs. VV is a double-stranded DNA virus with a large genome that replicates in cytoplasmic viral factories, where it imports ribosomes to produce viral proteins (26–28).

We compared the codon usages of IAV and VV to the codon usage of their human host (Figure 1). Codon usage can be expressed as either frequency per 1000 codons or relative synonymous codon usage (RSCU). Frequency per 1000 codons allows for comparison between species by adjusting for differences in coding sequence length. RSCU is a normalized index of codon usage that adjusts both for coding sequence length and amino acid composition. It has a value of 0 for unused synonymous codons, a value of 1 for equally used synonymous codons and a maximum of n, where n is the number of synonymous codons in the codon family. Regardless of the index used, the codon usages of IAV and VV correlate poorly with the codon usage of their human host. When codon usage is expressed as frequency per 1000, the R^2 correlation coefficient between viral and human codon usage is 0.26 for IAV and 0.01 for VV. When codon usage is expressed as RSCU, the the R^2 correlation coefficient is 0.10 for IAV and 0.08 for VV.

Analysis of tRNA abundance upon viral infection

Because host codon usage generally reflects the host tRNA (1,2,29–31), poor viral codon adaptation is thought to result in inefficient translation of viral genes. This assumes that rare host tRNAs are limiting in the translation of viral genes, and that the host tRNA pool remains unchanged after viral infection. There is extensive experimental evidence supporting the first assumption. Indeed, codon optimization has been shown to result in increased translation and greater immunogenicity of several viruses and bacteria (12–17). To our knowledge, however, previous studies have not explored whether viruses alter tRNA pools to favor translation of viral genes.

To address this question, we examined the changes in tRNA populations after infection with IAV or VV using tRNA microarray technology (18,21,32). For this study, we used custom-printed microarrays containing 37 probes for human nuclear-encoded tRNAs and 22 probes for human mitochondrial-encoded tRNAs. The arrays include 75 probes for *S. cerevisiae* tRNAs and 34 probes for *E. coli* tRNAs that serve as hybridization and specificity controls. We isolated total or polysome-associated RNA from cells 6 h post-infection. After selectively labeling tRNAs by ligation to a fluorophore-containing oligonucleotide, we hybridized the samples directly onto the microarray. We included an uninfected control sample in all array hybridizations to correct for variations in labeling and array manufacturing. The tRNA microarray method typically measures changes in tRNA levels relative to the control sample, so only relative tRNA levels were analysed in this study.

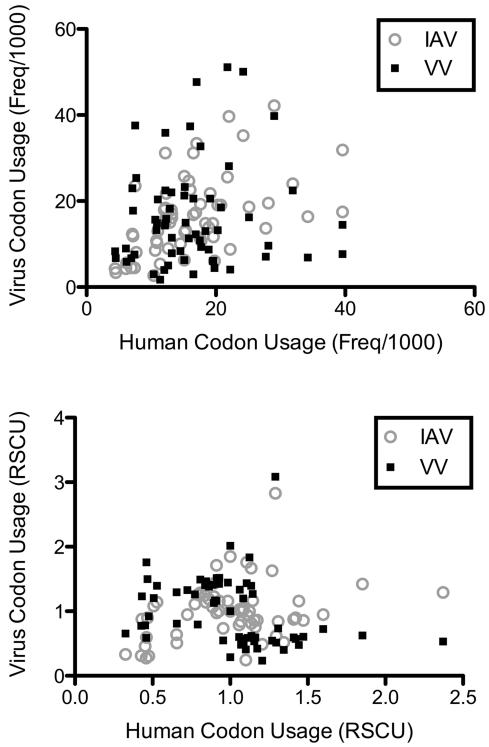

Figure 1. Codon usage of virus compared with human. Viral codon usage (IAV in gray, VV in black) is plotted against human codon usage. Codon usage is expressed as frequency per 1000 codons (top) or RSCU (bottom). Regardless of the index used, viral codon usage correlates poorly with human codon usage. When codon usage is expressed as frequency per 1000, the R^2 correlation coefficient between viral and human codon usage is 0.26 for IAV and 0.01 for VV. When codon usage is expressed as RSCU, the R^2 correlation coefficient is 0.10 for IAV and 0.08 for VV.

We first quantitated total nuclear- and mitochondrial-encoded tRNAs in virus-infected and uninfected cells. This revealed that infection with neither VV nor IAV alters global tRNA levels (Figure 2A, left panel). Similarly, for individual tRNA species, infection with either virus did not significantly alter abundance (Figure 2B, top). We conclude that cellular tRNA levels are not greatly altered by IAV- or VV-infection.

We then examined tRNA levels in polysome-associated RNA samples (for simplicity, polysome-associated RNA is termed polysome RNA in the text below). Polysome RNA was isolated from sucrose gradient polysome fractions, and therefore contains ribosome-bound tRNAs and tRNAs associated with aminoacyl synthetases and other components of the translation machinery (33). As expected, we detected only nuclear-encoded tRNAs but no mitochondrial-encoded tRNAs in polysome RNA samples (Figure 2A, right panel). As with cellular RNA samples, we found no significant difference in median polysome tRNA levels between IAV- or VV-infected versus uninfected cells. We observed, however, significant changes in individual polysome tRNA levels in virus-infected compared with uninfected cells (Figure 2B, bottom). IAV- and VV-infected cells each exhibit distinct changes in their polysome tRNA populations compared with uninfected control cells. For example, $tRNA^{Arg(UCU)}$ is most over-represented (1.6-fold) and $tRNA^{Gly(GCC/CCC)}$ is most under-represented (0.8-fold) in polysome RNA of IAV-infected cells. $tRNA^{Ile(UAU)}$ is most over-represented (2.4-fold) and $tRNA^{Arg(CCG/UCG)}$ is most under-represented (0.4-fold) in polysome RNA of VV-infected cells.

We conclude that the polysome tRNA population is selectively and significantly altered by IAV and VV infection, in contrast to total tRNA populations, which are not detectably altered.

tRNA—codon usage correlation analysis

IAV or VV infections alter the polysome tRNA population, most likely as a result of viral protein synthesis at the expense of host translation (34). To quantitate the contribution of virus versus host translation, we analysed protein synthesis 6 h post-infection by SDS-PAGE of total lysates from cells labeled for 5 min pulse with S^{35}-Met. This clearly revealed synthesis of major IAV or VV proteins superimposed on major inhibition of host protein synthesis: host shutdown was more complete with VV (Figure 3A). IAV-infected cells exhibited a higher total translation (1.5-fold) relative to VV-infected or uninfected cells (Figure 3B).

To correlate polysome tRNA levels with viral codon usage we plotted the relative tRNA levels versus the normalized codon usage of the virus (Figure 3C). For a given codon, the normalized codon usage is defined as the viral codon usage divided by the human codon usage. This normalization was necessary to allow direct comparison to the relative tRNA levels measured by microarray. We found that polysome tRNA levels correlate remarkably well with normalized viral codon usage: $R^2 = 0.57$ for IAV and $R^2 = 0.82$ for VV. The higher correlation coefficient obtained with VV is consistent with a greater proportion of viral translation relative to host translation, clearly seen by SDS-PAGE analysis (Figure 3A).

Viral adaptation for replication in IFN-exposed cells?

Though viral codon usage is poorly adapted to the HeLa tRNA pool, IAV and VV do not alter cellular tRNA levels to favor translation of their viral genes. Given the rapidity of infectious cycles of IAV and VV and the large size of tRNA pools ($\sim 5 \times 10^7$ copies of tRNA per cell) it may simply not be possible for viruses to acutely alter tRNAs to their benefit. Viruses, however, with longer infectious times may profit by modulating tRNA transcription to better match viral codon usage. Indeed, van Weringh *et al.* (35) proposed just this mechanism to account for the selective incorporation of normally low abundance tRNAs into HIV particles.

Under normal infection conditions, hosts will rapidly produce interferons (IFNs). Later rounds of viral replication will then occur in cells reprogrammed by IFNs. We recently reported that both type I and type II IFNs markedly change tRNA aminoacylation levels in HeLa cells (25). As seen in Figure 4A, IFN-γ generally increases tRNA expression, whereas IFN-β generally decreases

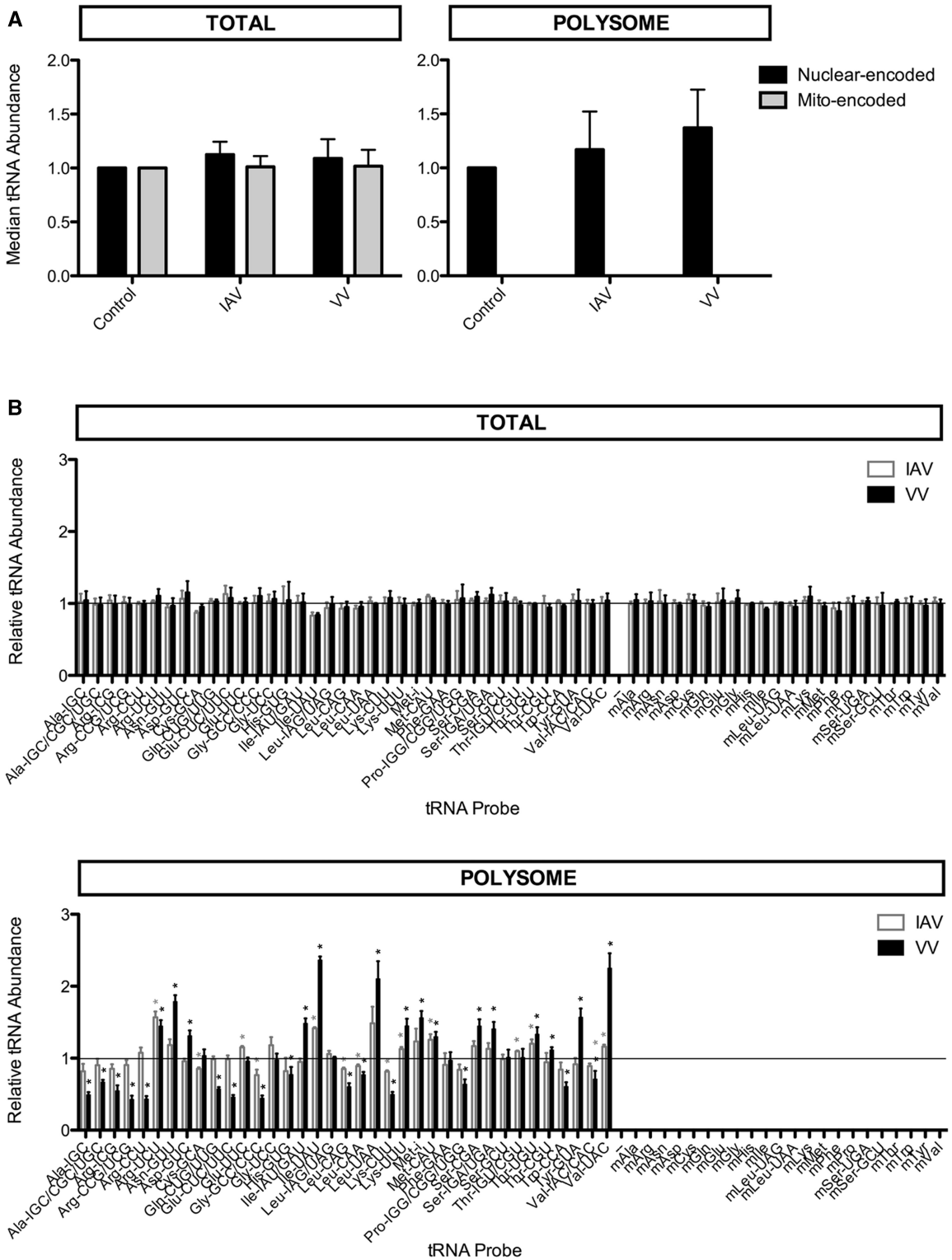

Figure 2. Changes in tRNA abundance after viral infection. HeLa cells were infected with IAV or VV; total cellular RNA or polysome RNA was isolated 6 h post-infection. tRNA abundance was measured by microarray relative to an uninfected control. Data are averages of three replicate experiments; error bars indicate standard deviation. (**A**) Median tRNA abundance after viral infection. Median values for nuclear-encoded tRNAs (black) and mitochondrial-encoded tRNAs (gray) are shown for IAV- and VV-infected cells relative to an uninfected control (set to 1). No mitochondrial-encoded tRNAs were detected in the polysome RNA samples. No significant changes in median tRNA abundance are detected in total cellular RNA (left) or polysome RNA (right). (**B**) Individual tRNA abundance after viral infection. Individual tRNA abundance values are shown for IAV (gray) and VV (black) infected cells relative to an uninfected control (set to 1, black line). A value of 1 indicates no change, a value <1 indicates a decrease and a value >1 indicates an increase after viral infection. No significant changes in individual tRNA abundances are detected in total cellular RNA (top), but distinct and virus-specific changes are observed in polysome RNA (bottom). One sample *t*-tests were performed to determine the statistical significance of the changes: * indicates *P*-value <0.0014 applying the Bonferroni correction for measuring multiple events (*P*-value/number of events, or 0.05/37).

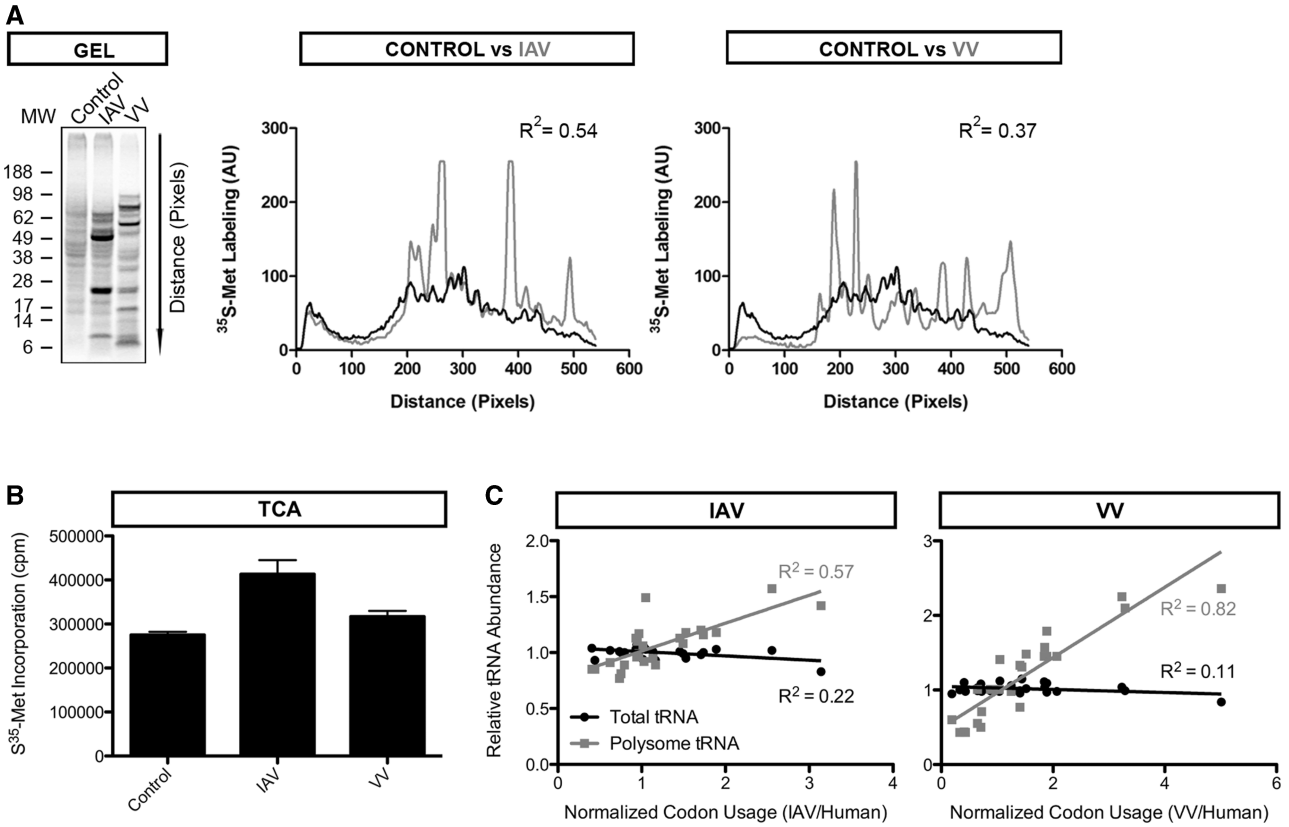

Figure 3. Polysome tRNAs reflect viral translation. (**A**) Translation patterns after viral infection. HeLa cells were infected with IAV, VV or mock-treated for the uninfected control. At 6 h post-infection, cells were pulsed with S^{35}-methionine and lysed. Cell lysate was loaded on an SDS-PAGE gel for visualization of S^{35}-labeled protein products (left). Signal intensity was quantitated to better compare the infected (IAV or VV) and the control samples (middle and right panels). Translation is significantly altered upon viral infection. However, VV is far more efficient than IAV in shutting down host translation (R^2 IAV/Ctrl > R^2 VV/Ctrl). (**B**) Quantitation of translation after viral infection. Cell lysate was obtained as in (A) and S^{35}-labeled protein products were quantitated on a scintillation counter after TCA precipitation. Values are averages of six technical replicates, error bars indicate standard deviation. A modest increase in translation is observed in IAV-infected cells but not VV-infected cells relative to the uninfected control. (**C**) tRNA—codon usage analysis. Relative tRNA abundance values after viral infection (IAV left, VV right) measured by microarray are plotted against normalized viral codon usage. Polysome tRNA values (gray) correlate well with viral codon usage, whereas total tRNA values (black) do not correlate with viral codon usage.

tRNA expression (these data were referred to, but not shown in (25)). For most viral codons, IFN exposure will have little positive or negative effect in matching cellular tRNA expression. Intriguingly, the only tRNA species commonly upregulated by type I and II IFNs is $tRNA^{Ile(UAU)}$, decoding the Ile-AUA codon which is the most overrepresented in the IAV and VV genomes (Figure 4B and C). This result suggests that evolution may have adapted IAV and VV Ile codons for better translation in IFN-γ-exposed cells.

CONCLUDING REMARKS

Since IAV and VV do not alter tRNA levels on the cellular scale, an intriguing possibility is the existence of local tRNA pools at sites of viral translation. tRNAs decoding codons rare in the host but frequent in the virus (such as Ile-AUA) may be recruited and re-used in successive rounds of viral translation, becoming enriched in the immediate environment. Such a 'channeled tRNA cycle' was first proposed by Deutscher *et al.* over 10 years ago: tRNAs are shuttled directly from the ribosome to their cognate tRNA synthetase and back to the ribosome for another round of translation, without reentering the cytosolic pool (36–38). Local tRNA pools would therefore be adapted to viral codon usage, enhancing translational efficiency of viral genes.

The possibility of local tRNA pools is particularly relevant in the case of VV, which replicates in cytoplasmic viral factories where the components of the translation machinery, including tRNA synthetases, are recruited (26,33). Clearly an area of future investigation is to study the local concentrations of individual tRNAs in VV-factories and at other locations of clearly compartmentalized translation. Although this can be approached experimentally by available techniques (such as FISH and introduction of labeled tRNAs into live cells), further technological advances will be required to finely discriminate between the myriad tRNA species and increase resolution.

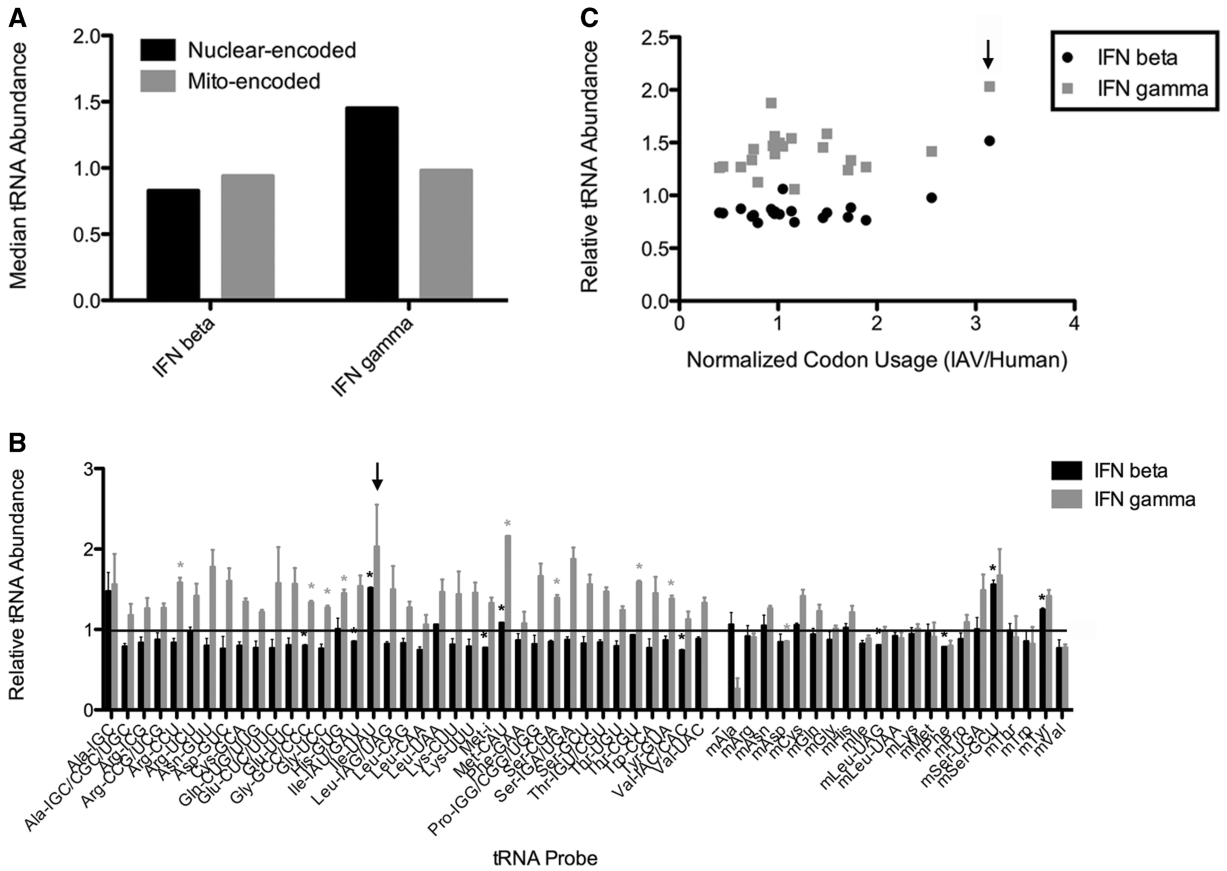

Figure 4. Changes in tRNA abundance after IFN treatment. HeLa cells were treated with IFN-β or IFN-γ for 16 h and total cellular RNA was isolated. tRNA abundance was measured by microarray relative to an untreated control. (**A**) Median tRNA abundance after IFN treatment. Median values for nuclear-encoded tRNAs (black) and mitochondrial-encoded tRNAs (gray) are shown for IFN-β or IFN-γ—treated cells relative to an untreated control (set to 1). IFN-β slightly decreases global nuclear-encoded tRNA levels, whereas IFN-γ treatment increases global nuclear-encoded tRNA levels. (**B**) Individual tRNA abundance after IFN treatment. Individual tRNA abundance values are shown for IFN-β (black) or IFN-γ (gray) treated cells relative to an untreated control (set to 1, black line). Data are averages from one dye-swapped experiment; error bars indicate standard deviation. A value of 1 indicates no change, a value <1 indicates a decrease and a value >1 indicates an increase after IFN treatment relative to untreated. $tRNA^{Ile(UAU)}$ is markedly increased upon IFN-β and IFN-γ treatment (black arrow). One sample *t*-tests were performed to determine the statistical significance of the changes: * indicates *P*-value <0.0009, applying the Bonferroni correction for measuring multiple events (*P*-value/number of events, or 0.05/58). (**C**) tRNA—codon usage analysis. Relative tRNA abundance values after IFN treatment (IFN-β in black and IFN-γ in gray) are plotted against normalized IAV codon usage. The Ile-AUA codon is over-represented in the IAV genome, correlating with an increase in $tRNA^{Ile(UAU)}$ abundance after IFN treatment (black arrow). Similar results are obtained when plotting against VV codon usage (not shown). These data were referred in (25) but not shown.

FUNDING

Division of Intramural Research, National Institute of Allergy and Infectious Diseases; National Institutes of Health [DP1 GM105386 to T.P.]. Funding for open access charge: Division of Intramural Research, National Institute of Allergy and Infectious Diseases.

Conflict of interest statement. None declared.

REFERENCES

1. Ikemura,T. (1981) Correlation between the abundance of Escherichia coli transfer RNAs and the occurrence of the respective codons in its protein genes: a proposal for a synonymous codon choice that is optimal for the E coli translational system. *J. Mol. Biol.*, **151**, 389–409.
2. Ikemura,T. (1985) Codon usage and tRNA content in unicellular and multicellular organisms. *Mol. Biol. Evol.*, **2**, 13–34.
3. Bahir,I., Fromer,M., Prat,Y. and Linial,M. (2009) Viral adaptation to host: a proteome-based analysis of codon usage and amino acid preferences. *Mol. Syst. Biol.*, **5**, 311.
4. Hilterbrand,A., Saelens,J. and Putonti,C. (2012) CBDB: the codon bias database. *BMC Bioinform.*, **13**, 62.
5. Roychoudhury,S., Pan,A. and Mukherjee,D. (2011) Genus specific evolution of codon usage and nucleotide compositional traits of poxviruses. *Virus Genes*, **42**, 189–199.
6. Ahn,I. and Son,H.S. (2012) Evolutionary analysis of human-origin influenza A virus (H3N2) genes associated with the codon usage patterns since 1993. *Virus Genes*, **44**, 198–206.
7. Wong,E.H., Smith,D.K., Rabadan,R., Peiris,M. and Poon,L.L. (2010) Codon usage bias and the evolution of influenza A viruses. Codon Usage Biases of Influenza Virus. *BMC Evol. Biol.*, **10**, 253.
8. Bulmer,M. (1991) The selection-mutation-drift theory of synonymous codon usage. *Genetics*, **129**, 897–907.
9. Palidwor,G.A., Perkins,T.J. and Xia,X. (2010) A general model of codon bias due to GC mutational bias. *PLoS ONE*, **5**, e13431.
10. Shah,P. and Gilchrist,M.A. (2011) Explaining complex codon usage patterns with selection for translational efficiency, mutation

bias, and genetic drift. *Proc. Natl Acad. Sci. USA*, **108**, 10231–10236.
11. Ma,M.R., Ha,X.Q., Ling,H., Wang,M.L., Zhang,F.X., Zhang,S.D., Li,G. and Yan,W. (2011) The characteristics of the synonymous codon usage in hepatitis B virus and the effects of host on the virus in codon usage pattern. *Virol. J.*, **8**, 544.
12. Carnero,E., Li,W., Borderia,A.V., Moltedo,B., Moran,T. and Garcia-Sastre,A. (2009) Optimization of human immunodeficiency virus gag expression by newcastle disease virus vectors for the induction of potent immune responses. *J. Virol.*, **83**, 584–597.
13. Shinoda,K., Wyatt,L.S., Irvine,K.R. and Moss,B. (2009) Engineering the vaccinia virus L1 protein for increased neutralizing antibody response after DNA immunization. *Virol. J.*, **6**, 28.
14. Tenbusch,M., Grunwald,T., Niezold,T., Storcksdieck Genannt Bonsmann,M., Hannaman,D., Norley,S. and Uberla,K. (2010) Codon-optimization of the hemagglutinin gene from the novel swine origin H1N1 influenza virus has differential effects on CD4(+) T-cell responses and immune effector mechanisms following DNA electroporation in mice. *Vaccine*, **28**, 3273–3277.
15. Wang,S., Farfan-Arribas,D.J., Shen,S., Chou,T.H., Hirsch,A., He,F. and Lu,S. (2006) Relative contributions of codon usage, promoter efficiency and leader sequence to the antigen expression and immunogenicity of HIV-1 Env DNA vaccine. *Vaccine*, **24**, 4531–4540.
16. Zhi,N., Wan,Z., Liu,X., Wong,S., Kim,D.J., Young,N.S. and Kajigaya,S. (2010) Codon optimization of human parvovirus B19 capsid genes greatly increases their expression in nonpermissive cells. *J. Virol.*, **84**, 13059–13062.
17. Zhao,K.N. and Chen,J. (2011) Codon usage roles in human papillomavirus. *Rev. Med. Virol.*, **21**, 397–411.
18. Dittmar,K.A., Goodenbour,J.M. and Pan,T. (2006) Tissue-specific differences in human transfer RNA expression. *PLoS Genet.*, **2**, e221.
19. Chen,W., Bocker,W., Brosius,J. and Tiedge,H. (1997) Expression of neural BC200 RNA in human tumours. *J. Pathol.*, **183**, 345–351.
20. Marshall,L. and White,R.J. (2008) Non-coding RNA production by RNA polymerase III is implicated in cancer. *Nat. Rev. Cancer*, **8**, 911–914.
21. Pavon-Eternod,M., Gomes,S., Geslain,R., Dai,Q., Rosner,M.R. and Pan,T. (2009) tRNA over-expression in breast cancer and functional consequences. *Nucleic Acids Res.*, **37**, 7268–7280.
22. Zhou,Y., Goodenbour,J.M., Godley,L.A., Wickrema,A. and Pan,T. (2009) High levels of tRNA abundance and alteration of tRNA charging by bortezomib in multiple myeloma. *Biochem. Biophys. Res. Commun.*, **385**, 160–164.
23. Kaufman,R.J. (2002) Orchestrating the unfolded protein response in health and disease. *J. Clin. Invest.*, **110**, 1389–1398.
24. O'Neill,L.A. and Bowie,A.G. (2010) Sensing and signaling in antiviral innate immunity. *Curr. Biol. CB*, **20**, R328–R333.
25. Netzer,N., Goodenbour,J.M., David,A., Dittmar,K.A., Jones,R.B., Schneider,J.R., Boone,D., Eves,E.M., Rosner,M.R., Gibbs,J.S. *et al.* (2009) Innate immune and chemically triggered oxidative stress modifies translational fidelity. *Nature*, **462**, 522–526.
26. Katsafanas,G.C. and Moss,B. (2007) Colocalization of transcription and translation within cytoplasmic poxvirus factories coordinates viral expression and subjugates host functions. *Cell Host Microbe*, **2**, 221–228.
27. David,A., Netzer,N., Strader,M.B., Das,S.R., Chen,C.Y., Gibbs,J., Pierre,P., Bennink,J.R. and Yewdell,J.W. (2011) RNA-binding targets aminoacyl-tRNA-synthetases to translating ribosomes. *J. Biol. Chem.*, **23**, 20688–20700.
28. David,A., Dolan,B.P., Hickman,H.D., Knowlton,J.J., Clavarino,G., Pierre,P., Bennink,J.R. and Yewdell,J.W. (2012) Nuclear translation visualized by ribosome-bound nascent chain puromycylation. *J. Cell Biol.*, **197**, 45–57.
29. Kanaya,S., Yamada,Y., Kinouchi,M., Kudo,Y. and Ikemura,T. (2001) Codon usage and tRNA genes in eukaryotes: correlation of codon usage diversity with translation efficiency and with CG-dinucleotide usage as assessed by multivariate analysis. *J. Mol. Evol.*, **53**, 290–298.
30. Novoa,E.M., Pavon-Eternod,M., Pan,T. and Ribas de Pouplana,L. (2012) A role for tRNA modifications in genome structure and codon usage. *Cell*, **149**, 202–213.
31. Ran,W. and Higgs,P.G. (2010) The influence of anticodon-codon interactions and modified bases on codon usage bias in bacteria. *Mol. Biol. Evol.*, **27**, 2129–2140.
32. Pavon-Eternod,M., Wei,M., Pan,T. and Kleiman,L. (2010) Profiling non-lysyl tRNAs in HIV-1. *RNA*, **16**, 267–273.
33. David,A., Netzer,N., Strader,M.B., Das,S.R., Chen,C.Y., Gibbs,J., Pierre,P., Bennink,J.R. and Yewdell,J.W. (2011) RNA binding targets aminoacyl-tRNA synthetases to translating ribosomes. *J. Biol. Chem.*, **286**, 20688–20700.
34. Bushell,M. and Sarnow,P. (2002) Hijacking the translation apparatus by RNA viruses. *J. Cell Biol.*, **158**, 395–399.
35. van Weringh,A., Ragonnet-Cronin,M., Pranckeviciene,E., Pavon-Eternod,M., Kleiman,L. and Xia,X. (2011) HIV-1 modulates the tRNA pool to improve translation efficiency. *Mol. Biol. Evol.*, **28**, 1827–1834.
36. Petrushenko,Z.M., Budkevich,T.V., Shalak,V.F., Negrutskii,B.S. and El'skaya,A.V. (2002) Novel complexes of mammalian translation elongation factor eEF1A.GDP with uncharged tRNA and aminoacyl-tRNA synthetase. Implications for tRNA channeling. *Eur. J. Biochem.*, **269**, 4811–4818.
37. Stapulionis,R. and Deutscher,M.P. (1995) A channeled tRNA cycle during mammalian protein synthesis. *Proc. Natl Acad. Sci. USA*, **92**, 7158–7161.
38. Mirande,M. (2010) Processivity of translation in the eukaryote cell: role of aminoacyl-tRNA synthetases. *FEBS Lett.*, **584**, 443–447.